Supporting information

Exploring the Stability and Catalytic Activity of Monoethanolamine Functionalized CuO Electrode in Electrochemical CO_2 Reduction

Jéssica C. de Almeida,[1] Osmando F. Lopes,[2] Meital Shviro,[3,#] Gelson T. S. T. da Silva,[4] Caue Ribeiro,[5*] and Vagner R. de Mendonça[1,6*]

1 - Federal University of São Carlos, Science and Technology Center for Sustainability, 18052-780, Sorocaba, SP, Brazil

2 - Laboratory of Photochemistry and Materials Science, Institute of Chemistry, Federal University of Uberlândia, Uberlândia, MG, Brazil

3 - Forschungszentrum Jülich GmbH, Institute of Energy and Climate Research: Electrochemical Process Engineering (IEK-14), 52425 Jülich, Germany.

4 - Interdisciplinary Laboratory of Electrochemistry and Ceramics, Department of Chemistry, Federal University of Sao Carlos, São Carlos, São Paulo, 13565-905, Brazil

5 - Nanotechnology National Laboratory for Agriculture (LNNA), Embrapa Instrumentation, 13561-206, São Carlos, SP, Brazil.

6 - Federal Institute of Education, Science, and Technology of São Paulo – IFSP Campus Itapetininga,18202-000, Itapetininga, SP, Brazil.

Current address: Chemistry and Nanoscience Center, National Renewable Energy Laboratory (NREL), Golden, CO 80401, USA

Corresponding authors: *vrm@ifsp.edu.br; caue.ribeiro@embrapa.br*

Experimental section

Characterization of the Materials

X-ray diffraction (XRD) The crystalline phases were characterized by X-ray diffraction (XRD) over the 2θ range from 20 to 80° using a Shimadzu XRD-6000 diffractometer operating with CuKα radiation. A Fourier Transform Infrared spectrometer (FTIR) (Bruker VERTEX 70) was used to investigate surface changes using ATR mode with 64 scans and 4 cm^{-1} resolution in the 4000 - 400 cm^{-1}. Sample morphology and particle size were analyzed by field emission gun scanning electron microscopy (FEGSEM) JEOL JSM 6701 F.

Raman spectroscopy was performed using a T64000 spectrometer (Horiba Jobin-Yvon, Japan) coupled with a Synapse CCD and an argon ion laser operating at 633 nm.

X-ray photoelectron spectroscopy (XPS) was employed to analyze the surface chemical composition of the catalyst materials. The analysis was performed using a Phi 5000 VersaProbe II instrument (ULVAC-PHI Inc., USA). The X-ray source was monochromatic Al Kα radiation (1.486 keV) with operating settings of 50 W power, 15 kV accelerating voltage, and a 200 μm spot size. Survey spectra were acquired using a pass energy of 187.5 eV, a step size of 0.8 eV, and a dwell time of 100 ms per step. Detailed high-resolution spectra were obtained using a pass energy of 23.5 eV, a step size of 0.1 eV, and a dwell time of 100 ms per step. The binding energy was referenced to the C 1s peak at 284.8 eV

N_2 adsorption-desorption isotherms were measured with a Micromeritics ASAP 2020 analyzer at 77 K. Samples were previously degassed at 80 °C under vacuum until a degassing pressure <10 μmmHg. The Brunauer–Emmett–Teller (BET) method was used to calculate the specific surface area (SSA). The zeta potential was measured at room temperature using a Zetasizer Nano-ZS analyzer (Malvern Instruments, UK), at natural pH.

Gas products (CO and H_2) were analyzed in a gas chromatography (PerkinElmer) coupled with a thermal conductivity detector (TCD), while the hydrocarbons (CH_4, C_2H_4) were identified and quantified by a gas chromatography (Shimadzu) coupled with a flame ionization detector (FID). Liquid products were quantified by 1 H nuclear magnetic resonance (NMR) (600 MHz, Ascend™ 600 Bruker) at 25 ◦C. The data were processed using the MestReNova software.

In the final stage of testing using an MEA cell, the anolyte was subjected to analysis by HPLC, Shimadzu model LC-20A, equipped with a Supelcogel C610H column (30 cm x 7.8 mm). Before injection, the sample was diluted and neutralized with a 2 M H_3PO_4 solution. The analysis was performed using an ultraviolet detector set at a wavelength of 210 nm. The eluent consisted of a 0.1 % aqueous H_3PO_4 solution, with a pump flow rate of 0.5 mL min^{-1} and a column oven temperature maintained at 32°C. The injection volume was 20 μL.

Diffuse reflectance infrared Fourier transform spectroscopy (DRIFTS) analysis of CO_2 adsorption and desorption was conducted using a Nicolet iS50 FTIR spectrometer equipped with a praying mantis accessory and a Harrick cell. Prior to CO_2 adsorption, the sample was subjected to a 20 mL min^{-1} He flow for 30 minutes at 25 °C. Subsequently, CO_2 was purged at a flow rate of 20 mL min^{-1} for the adsorption process. Following this, the He flow was reinstated for 10 minutes to observe CO_2 desorption. Spectra were collected every minute during adsorption and desorption at a resolution of 4 cm^{-1} and averaged over 32 scans. Samples were diluted to 5% mass in KBr. To measure the GDE, the electrode was bisected, and one half was subjected to electrochemical CO2 reduction in an MEA cell at a current density of 50 mA cm^{-2}. The catalyst layer of the GDEs was then scraped off, diluted to 5% mass in KBr, and analyzed using DRIFTS

Scherrer equation

XRD measurements were used to calculate the average crystallite size of the samples by the Scherrer equation (1), as follows [1]:

$$D = \frac{K\,\lambda}{\beta \cos\theta}$$

Where k is the Scherrer constant (0.9), λ is the wavelength of the X-ray radiation (1.5406 Å), β is the full width at half maximum of the diffraction peak at 2θ, and θ is the Bragg angle in radians.

Faradaic efficiency calculations

$$FE(\%) = \frac{n_x . n_{e^- x} . F}{Q}$$

Where x is a specific product, n_x is the amount of product x (mol), $n_{e^- x}$ is the number of needed electrons to produce x, F is the Faraday constant (94 685 C/mol), and Q is the total charge.

Results and discussion

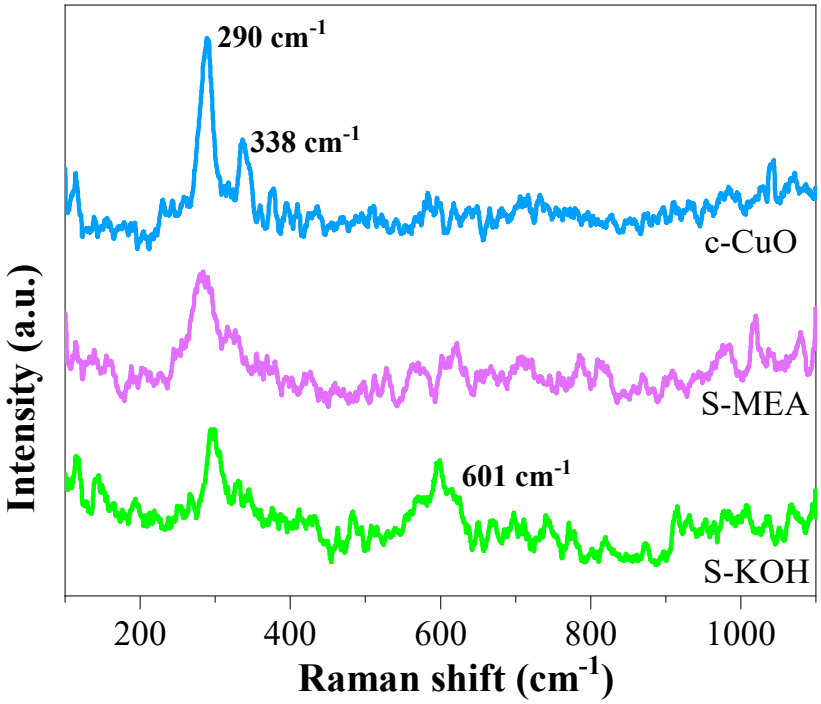

Figure S1. Raman spectra of samples c-CuO, S-MEA, and S-KOH.

FTIR of S-KOH and S-MEA in Figure S2 show characteristic Cu(II)-O band within the 400 to 600 cm^{-1} range. [2] The samples demonstrate asymmetric and symmetric stretching bands of C=O at 1561 cm^{-1} and 1391 cm^{-1}, respectively, indicative of acetate residues from the synthesis process. [3] The S-MEA spectra, exhibit bands at 3415 and 2979 cm^{-1}, assigned to N-H bonds [3–5] originating from MEA functional groups, providing strong evidence for surface functionalization. The s-KOH sample presents an OH band at 3228 cm^{-1}.

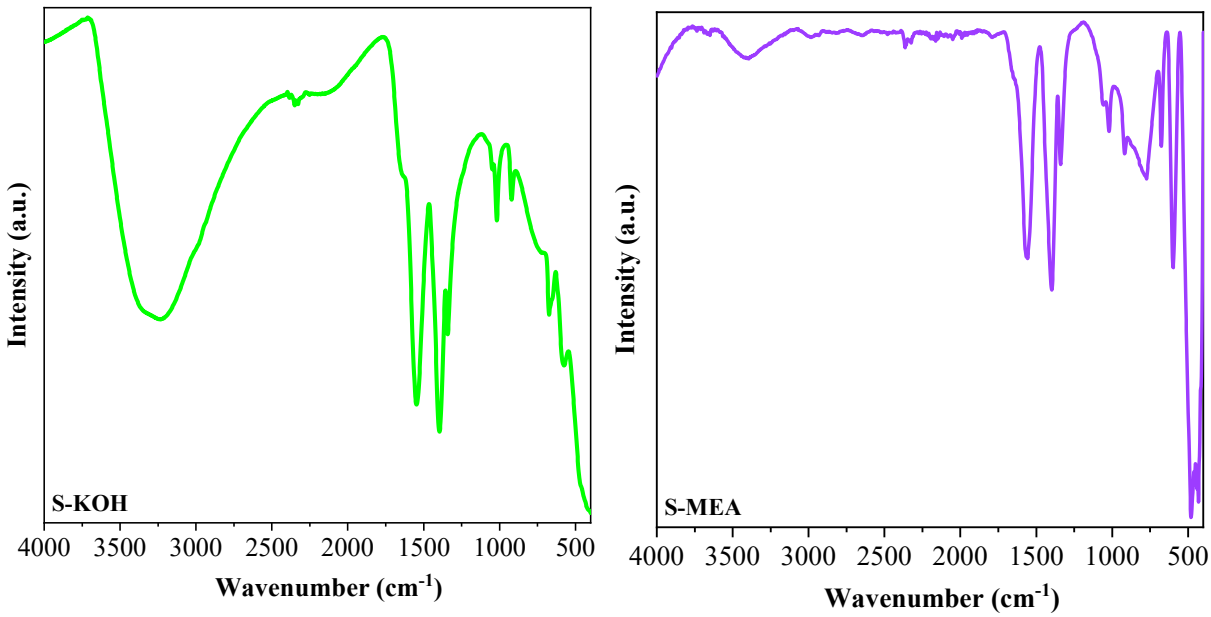

Figure S2. FTIR spectra of samples S-KOH and S-MEA.

For the S-KOH sample in Figure S3a, characteristic Cu and O peaks are prominent at approximately 930 eV for Cu $2p^3$ and between 800 to 550 eV for Cu LMM, with Cu 3s and Cu 3p peaks appearing at around 115 eV and 90 eV, respectively. Peaks corresponding to O 1s and O KLL are noted at approximately 525 eV and 970 eV, respectively. [6] Additionally, the spectrum also shows the presence of K, derived from the KOH, and C from the equipment calibration. The XPS spectrum from the S-MEA sample in Figure S3b reveals, that apart from the characteristic Cu and O peaks, the presence of N originated from monoethanolamine constituting 0.8% of the atomic composition. The energy spectrum of Cu $2p^3$ and O 1s corroborates with XRD and FTIR data, confirming the CuO catalysts composition.

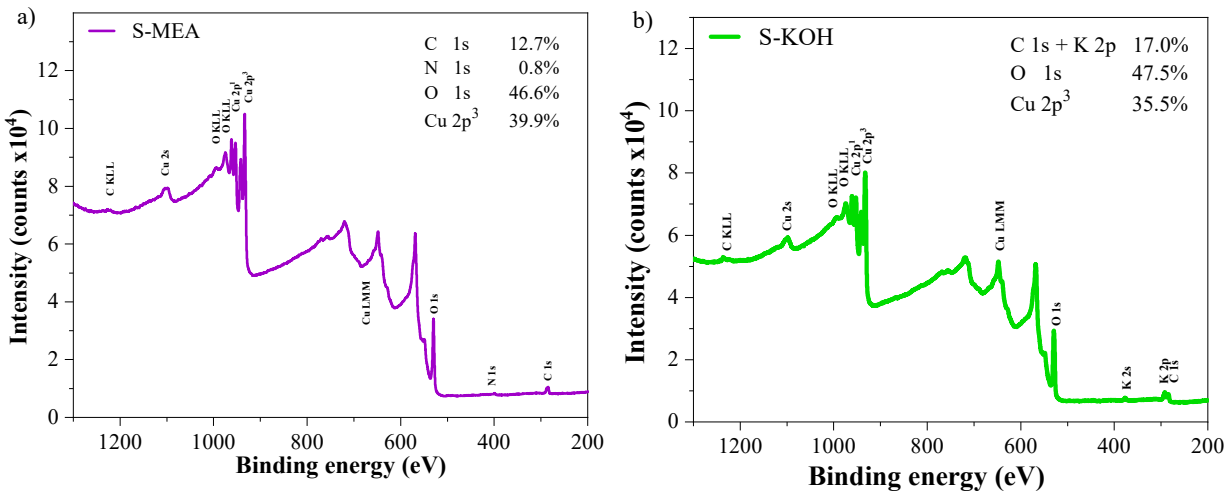

Figure S3. X-ray photoelectron survey spectra of S-MEA in (a) and S-KOH catalysts in (b) and high-resolution spectra of O 1s of S-MEA in (c) and S-KOH in (d).

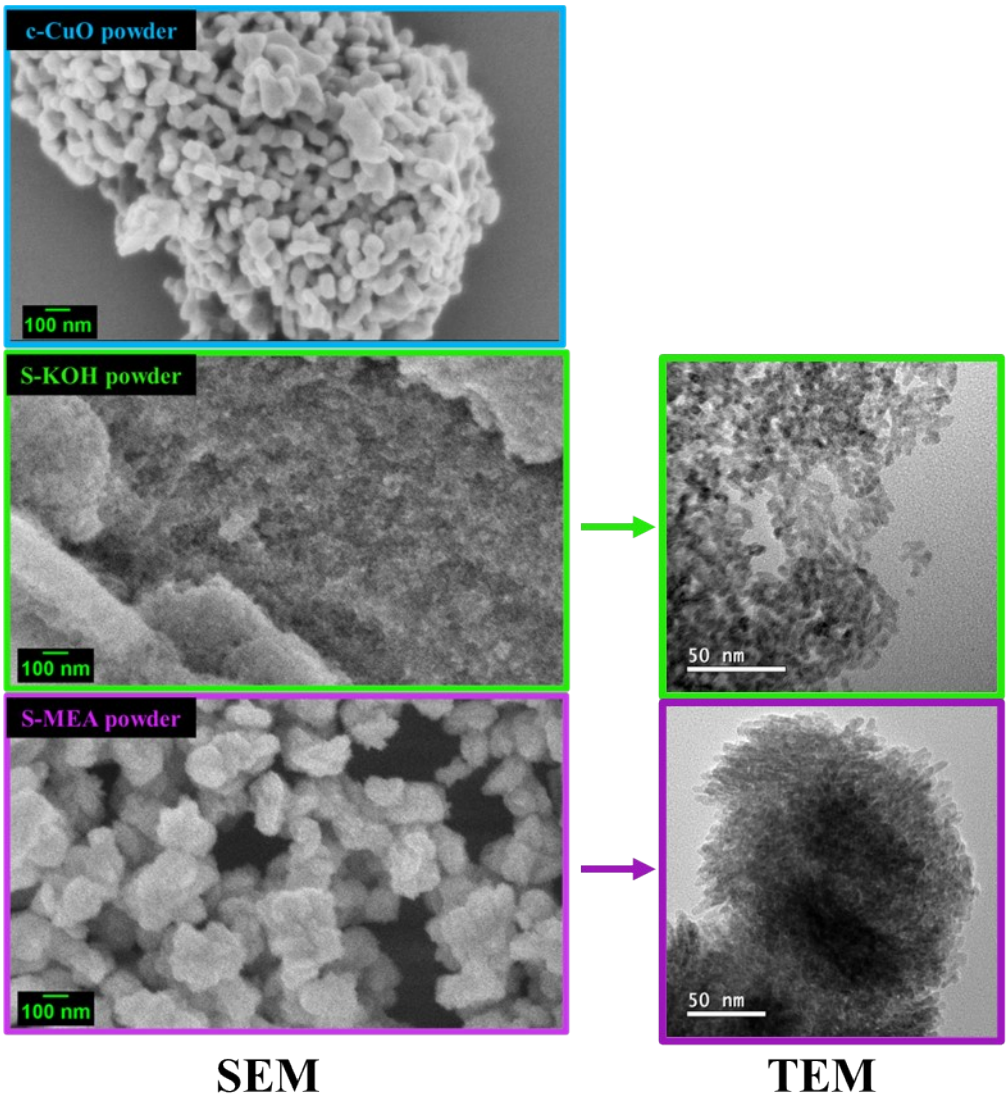

Figure S4. SEM images of the c-CuO, S-KOH, and S-MEA catalyst powders, along with TEM images of the S-KOH and S-MEA samples.

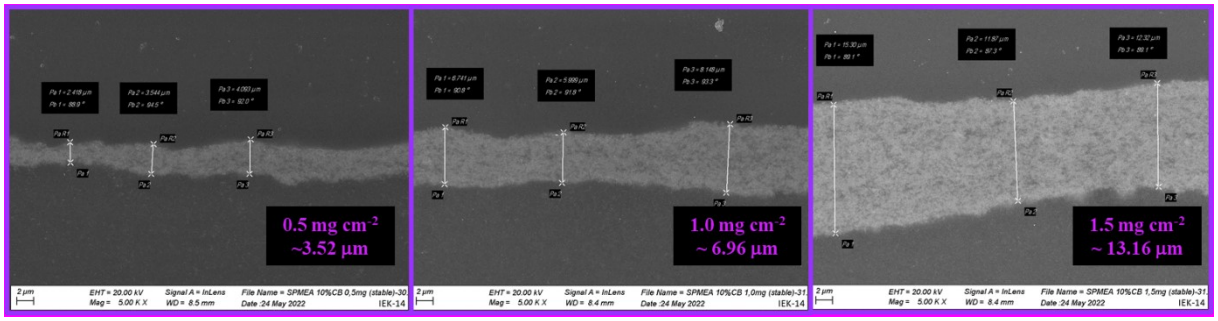

Figure S5. Cross-section images of the deposited layer of S-MEA with 10% carbon black on the carbon paper surface, with the indication of the load and the average thickness of each layer.

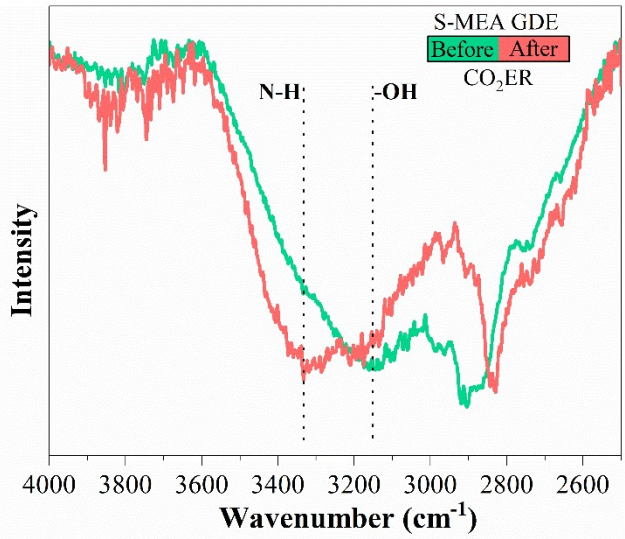

Figure S6. FTIR spectra of S-MEA GDE before and after a 20-minute electrochemical CO2 reduction test in a membrane electrode assembly cell.

References:

1 J. C. de Almeida, M. T. Corrêa, R. H. Koga, D. M. S. Del Duque, O. F. Lopes, G. T. S. T. da Silva, C. Ribeiro and V. R. de Mendonça, *New J. Chem.*, 2020, **44**, 18216–18224.

2 T. X. Wang, S. H. Xu and F. X. Yang, *Powder Technology*, 2012, **228**, 128–130.

3 M. A. Badillo-Ávila, R. Castanedo-Pérez, M. A. Villarreal-Andrade and G. Torres-Delgado, *Materials Science in Semiconductor Processing*, 2018, **85**, 168–176.

4 A. Dastneshan, S. Rahiminezhad, M. Naderi Mezajin, H. Nouri Jevinani, I. Akbarzadeh, M. Abdihaji, R. Qahremani, M. Jahanbakhshi, Z. Asghari Lalami, H. Heydari, H. Noorbazargan and E. Mostafavi, *Chemical Engineering Journal*, 2023, **455**, 140544.

5 F. S. Mjalli, G. Murshid, S. Al-Zakwani and A. Hayyan, *Fluid Phase Equilibria*, 2017, **448**, 30–40.

6 R. P. Vasquez, *Surface Science Spectra*, 1998, **5**, 262–266.